IET Communications

Research Article

IET Journals
The Institution of Engineering and Technology

Optimal sensing interval in cognitive radio networks with imperfect spectrum sensing

ISSN 1751-8628
Received on 31st March 2015
Accepted on 8th October 2015
doi: 10.1049/iet-com.2015.0671
www.ietdl.org

Boyang Liu ✉, *Zan Li, Jiangbo Si, Fuhui Zhou*

Integrated Service Networks Laboratory, Xidian University, Xi'an, People's Republic of China
✉ *E-mail: boyangliulby@163.com*

Abstract: Spectrum sensing is performed at the beginning of each time slot in traditional cognitive radio networks, which is unreasonable and needless since the presence or the absence of a primary user (PU) always lasts several time slots. A hidden Markov model is used to describe the imperfect spectrum sensing process over Rayleigh fading channels. On the basis of the sensing results, a hybrid interweave/underlay mode is exploited by the secondary user (SU) to achieve a higher throughput. To solve the tradeoff problem among the average energy consumption for spectrum sensing, the average throughput of SU and the average interference to the PU, an optimisation problem is proposed. The optimal sensing interval to determine when the next spectrum sensing should be performed is obtained by solving the optimisation problem. Numerical results are given to verify the authors' analysis.

1 Introduction

As the explosive growth of wireless communications in recent years, the radio spectrum has become a limited resource. It is theoretically impossible to obtain higher spectrum utilisation by modulation and coding, which approach the Shannon limits [1]. Although the usable spectrum is limited, a large portion of the licensed spectrum is severely underutilised. Federal Communications Commission (FCC) states that the utilisation of the assigned spectrum only ranges from 15 to 85% [2]. Motivated by this fact, cognitive radio (CR) has been proposed in [3, 4]. In CR systems, secondary users (SUs) are permitted to access the temporally unused bands of a primary user (PU). In this regard, a critical aspect of CR is the ability to sense the channels of the PU for unused portions. Therefore, spectrum sensing plays a crucial role in CR systems.

The most common spectrum sensing algorithms for CR systems are matched filter detection, energy detection, cyclostationary detection and eigenvalue-based detection [5–10]. Each of these methods has its own operational requirements, advantages and disadvantages. Moreover, many spectrum sensing schemes have been proposed to incorporate cooperation among the SU nodes to improve the sensing performance [11–13]. In CR systems, the SU is permitted to access the spectrum in three fashions: interweave, underlay and overlay [14, 15]. In interweave mode, which is the most popular one in the literature, the SU can transmit its message only when it senses the PU to be idle. In underlay mode, an interference power constraint is imposed on the SU's transmit power to protect the PU's transmission. In overlay mode, the SU uses sophisticated signal processing and coding technology to enhance the PU's throughput and obtain some additional bandwidth for its own transmission.

Traditionally, in a time-slotted CR system, spectrum sensing is performed at each time slot. However, according to many studies [16–18], the activities of the PU are not random. The duration of a PU's state (idle or active) usually lasts a number of time slots. Therefore, performing spectrum sensing at each slot not only wastes energy, but also losses opportunities for the SU to transmit signal (the SU can use the time devoted to spectrum sensing to transmit data). Hence, there arises a need for optimally choosing a spectrum sensing interval: the time interval (the number of time slots) during which the current state of the PU is considered to remain unchanged and no further spectrum sensing is needed [17]. Notice that if the sensing interval is too long, the energy consumed for spectrum sensing would be conserved, but the SU may miss many transmission opportunities (when the current state of the PU is active), or it may generate more interference to the PU (when the current state of the PU is idle). Therefore, it is important to create the tradeoff among the secondary throughput, the energy consumption for spectrum sensing and the interference to the PU.

Hidden Markov model (HMM) has widely been used in the field of speech processing. A review of HMM can be found in [19]. In the context of CR, many researchers use HMM to perform spectrum sensing [20–22]. The existence of a Markov chain in the channel utilisation of the PU over the time domain has been validated [18]. In this paper, we employ an HMM as a framework to model the behaviour of the SU. To make full use of the spectrum source, we use a hybrid interweave/underlay mode, i.e. the SU uses interweave mode if the current sensing result is idle, otherwise, underlay mode will be used. When the current sensing result is active, we calculate the average throughput of the SU, the average decreased throughput of the SU and the average energy consumption for spectrum sensing of the SU. When the current sensing result is idle, the average interference to the PU, the average throughput of the SU and the average energy consumption for spectrum sensing of the SU are calculated. An user satisfaction degree based on the sigmoid function is used to combine all the aforementioned factors. The optimal spectrum sensing interval is the number of slots to maximise the satisfaction degree of the SU. The closest published paper to our work is [17]. However, in [17], spectrum sensing is assumed to be perfect. We focus on the imperfect spectrum sensing which is the most practical aspect of CR systems. Moreover, the system model and the object function of [17] are different from ours. The effect of the system parameters on the spectrum sensing interval is investigated in the simulation.

The rest of this paper is organised as follows. The system model is presented in Section 2. In Section 3, an optimisation problem is formulated to obtain the optimal spectrum sensing interval. Simulation results and discussions are given in Section 4. In Section 5, we conclude the paper. Finally, the proofs of the derived expressions are given in Appendices 1 and 2.

2 System model

2.1 Channel model

Consider a CR network comprised of a pair of primary transmitter and receiver u and v, and a pair of secondary communication nodes s and d, as depicted in Fig. 1. The CR network is assumed

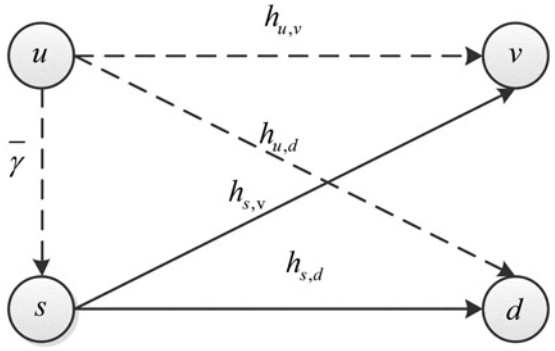

Fig. 1 *Channel model*

to operate in time-slotted mode with slot length T and the SU slots are synchronised to the PU slots. Let $h_{s,v}$, $h_{s,d}$, $h_{u,v}$ and $h_{u,d}$ denote the channel coefficients from s to v, from s to d, from u to v and from u to d, respectively. All these channels are assumed to subject to pairwise independent Rayleigh fading with additive white Gaussian noise (AWGN). Therefore, the instantaneous channel power gains, $|h_{s,v}|^2$, $|h_{s,d}|^2$, $|h_{u,v}|^2$ and $|h_{u,d}|^2$ are of exponential distribution with means $\sigma_{s,v}^2$, $\sigma_{s,d}^2$, $\sigma_{u,v}^2$ and $\sigma_{u,d}^2$, respectively. It is assumed that $\sigma_{s,v}^2 = \sigma_{s,d}^2 = \sigma_1^2$, $\sigma_{u,v}^2 = \sigma_{u,d}^2 = \sigma_2^2$ and the channel coefficients remain constant during a time slot, but change from one slot to another for each wireless link. Spectrum sensing is performed at the secondary transmitter (ST) and the channel between u and s is also Rayleigh fading with the average received average signal-to-noise ratio (SNR) (when the PU is active) $\bar{\gamma}$. The power of the AWGN is N_0, which is assumed to be the same for all channels.

2.2 Hidden Markov model

The spectrum sensing process can be modelled as an HMM, as shown in Fig. 2. Hypothesis $H_0\{q_k = 0\}$ (PU's state is idle) and $H_1 \triangleq \{q_k = 1\}$ (PU's state is active) denote the absence of a PU transmission in slot k and the existence, respectively. The prior probabilities of the two states are $P(H_0)$ and $P(H_1)$. $P_d = P(H_1|H_1.)$ and $P_f = P(H_1|H_0.)$ denote the detection and false alarm probabilities, respectively. The PU's transmission is modelled as a two-state homogeneous Markov process with the state space $X = \{x_1, x_2\}$, where $x_1 = 0$, $x_2 = 1$. These states are hidden since they are not directly observable (due to the influence of the AWGN and the channel fading). The SU senses the channel of the PU and obtains its observation result o_t, which is the SU's local decision for slot t. The observation state space is $Y = \{y_1, y_2\}$, where $y_1 = 0$, $y_2 = 1$.

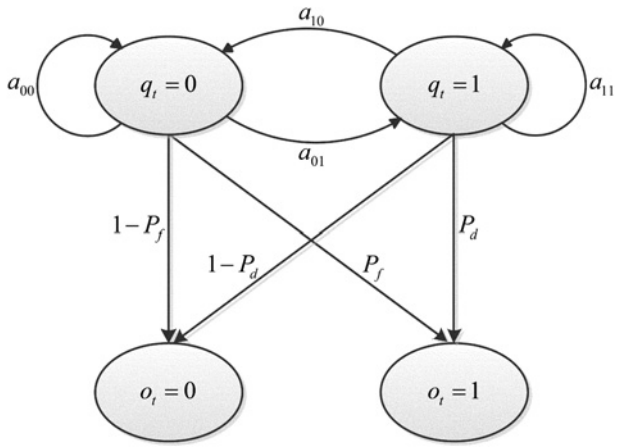

Fig. 2 *Hidden Markov model*

An HMM can be denoted by $\lambda = (\boldsymbol{\pi}, \boldsymbol{A}, \boldsymbol{B})$, where $\boldsymbol{\pi}$ is the initial state distribution: $\boldsymbol{\pi} = \{\pi_i\}$, $\pi_i = P(q_1 = i)$, $i \in X$; $\boldsymbol{A}$ is the state transition probability matrix: $\boldsymbol{A} = \{a_{ij}\}$, $a_{ij} = P(q_{t+1} = j|q_t = i.)$, $i, j \in X$; $\boldsymbol{B}$ is emission probability matrix: $\boldsymbol{B} = \{b_{jk}\}$, $b_{jk} = P(o_t = k|q_t = j.)$, $j \in X$, $k \in Y$. In our sensing scenario, $\pi_i = P(H_i)$, $i \in X$, $b_{jk} = P(H_k|H_j.)$, $j \in X$, $k \in Y$.

3 Optimal sensing interval

3.1 Algorithm for HMM parameter estimation

The parameters of the HMM are determined by solving the following optimisation problem, given as [17, 19]

$$\widehat{\lambda} = \left(\widehat{\boldsymbol{\pi}}, \widehat{\boldsymbol{A}}, \widehat{\boldsymbol{B}}\right) = \arg \max_{(\boldsymbol{\pi}, \boldsymbol{A}, \boldsymbol{B})} P(\boldsymbol{O}|\lambda) \tag{1}$$

where $P(\boldsymbol{O}|\lambda)$ is the probability of the observation sequence $\boldsymbol{O} = \{o_t\}_{t=1}^M$. In order to solve (1), a training phase is needed. In AWGN channel, the channel gain is fixed, at the beginning of the training, the ST senses the PU for M consecutive slots to obtain the decision sequence $\boldsymbol{O} = \{o_t\}_{t=1}^M$ (observation sequence or training sequence), where $o_t \in \{0, 1\}$ is the decision made by ST at slot t. However, when the channel gain follows Rayleigh fading distribution, each element of the observation sequence $\boldsymbol{O} = \{o_t\}_{t=1}^M$ is obtained under different channel conditions (channel gain), which is equivalent to the case that each o_t corresponding a new PU. Therefore, in AWGN channel, the training sequence can be obtained without the PU's any prior knowledge, while for the Rayleigh channel, the states of the PU's first M consecutive slots must be known, which constitute the training sequence. The training algorithm of HMM is an iterative algorithm, which is given as [19, 23]

$$\alpha_t(i) = \left[\sum_{j \in X} \alpha_{t-1}(j) a_{ji}\right] b_{io_t}, \quad t = 1, 2, \ldots, M, \ i \in X \tag{2}$$

$$P(\boldsymbol{O}|\lambda) = \sum_{i \in X} \alpha_{M-1}(i) \tag{3}$$

$$\beta_t(i) = \sum_{j \in X} a_{ij} b_{jo_{t+1}} \beta_{t+1}(j), \quad t = M-1, M-2, \ldots, 1, \ i \in X \tag{4}$$

$$\Theta_t(i, j) = \frac{\alpha_t(i) a_{ij} b_{jo_{t+1}} \beta_{t+1}(j)}{P(\boldsymbol{O}|\lambda)}, \quad i, j \in X \tag{5}$$

$$\Theta_t(i) = \sum_{j \in X} \Theta_t(i, j), \quad i \in X \tag{6}$$

$$\pi_i = \Theta_1(i), \quad i \in X \tag{7}$$

$$a_{ij} = \frac{\sum_{t=1}^{M-1} \Theta_t(i, j)}{\sum_{t=1}^{M-1} \Theta_t(i)}, \quad i, j \in X \tag{8}$$

$$b_{jk} = \frac{\sum_{o_t = k, t \in \{1, 2, \ldots, M-1\}} \Theta_t(j)}{\sum_{t=1}^{M-1} \Theta_t(j)}, \quad j \in X, \ k \in Y \tag{9}$$

where $\alpha_t(i)$ and $\beta_t(i)$ are forward and backward partial likelihoods, respectively. The iteration is initialised by setting $\pi_i = 1/2$, $i \in X$, $b_{jk} = 1/2$, $j \in X$, $k \in Y$, $\alpha_1(i) = \pi_i b_{io_1}$, $\beta_M(i) = 1$, $i \in X$. The iteration process might be desirable to stop if $P(\boldsymbol{O}|\lambda)$ does not increase by at least some predetermined threshold and/or to set a maximum number of iterations [23]. The estimation accuracy of the PU's parameters depends on the length of the training sequence M. As HMM training is not a key point in our work, we assume that the M is large enough to achieve enough estimation accuracy and the error of estimation can be ignored. The number of iterations is

IET Commun., 2016, Vol. 10, Iss. 2, pp. 189–198

generally not large. Therefore, the complexity of the HMM algorithm is $O(M)$.

3.2 Problem formulation

Energy detector is used to perform spectrum sensing. The average detection probability and false alarm probability of energy detector over Rayleigh fading channel are given by [24]

$$P_{\mathrm{d}} = P\left(H_1 \middle| H_1\right) = \mathrm{e}^{-\theta/2} \sum_{n=0}^{N_s-2} \frac{1}{n!} \left(\frac{\theta}{2}\right)^n + \left(\frac{1+\bar{\gamma}}{\bar{\gamma}}\right)^{N_s-1} \left[\mathrm{e}^{-\theta/2(1+\bar{\gamma})} - \mathrm{e}^{-\theta/2} \sum_{n=0}^{N_s-2} \frac{1}{n!} \frac{\theta\bar{\gamma}}{2(1+\bar{\gamma})}\right] \tag{10}$$

$$P_{\mathrm{f}} = \frac{\Gamma\left(N_s, \theta/N_0\right)}{\Gamma\left(N_s\right)} \tag{11}$$

where θ is the decision threshold. N_s is the number of samples collected during sensing time at one slot and $\overline{\gamma}$ is the average SNR. $\Gamma(\cdot)$ and $\Gamma(\cdot,\cdot)$ are the gamma functions [25, Eq. 8.310.1] and incomplete gamma function [25, Eq. 8.350.2], respectively.

As we employ the hybrid interweave/underlay mode, the transmit power of the SU is determined by

$$P_s = \begin{cases} P_{\max}, & \widehat{H} = H_0 \\ \min\left(P_{\max}, \dfrac{I}{\left|h_{s,v}\right|^2}\right), & \widehat{H} = H_1 \end{cases} \tag{12}$$

where I is the interference power constraint of the PU. $P_{\max}$ is the maximum transmit power of the SU and $\widehat{H}$ is the sensing result of the SU. The received SNR/SINR at d is expressed as

$$\gamma_{\mathrm{d}} = \frac{P_s\left|h_{s,d}\right|^2}{\psi P_u\left|h_{u,d}\right|^2 + N_0} \tag{13}$$

where ψ is defined as

$$\psi = \begin{cases} 0, & H_{\mathrm{true}} = H_0 \\ 1, & H_{\mathrm{true}} = H_1 \end{cases} \tag{14}$$

where H_{true} denotes the current true state of the PU. Similar to [26], we consider the scenario that the influence of the influence of the noise at the receiver d is negligible compared to that of the interference signals. Hence, we have

$$\gamma_d = \begin{cases} \dfrac{P_s\left|h_{s,d}\right|^2}{N_0}, & \psi = 0 \\ \dfrac{P_s G_1}{P_u}, & \psi = 1 \end{cases} \tag{15}$$

where $G_1 = |h_{s,d}|^2/|h_{u,d}|^2$ is a random variable with probability density function (PDF) $f_{G_1}(g_1)$, which is given by [27]

$$f_{G_1}(g_1) = \frac{\sigma_1^2\sigma_2^2}{\left(\sigma_1^2 + \sigma_2^2 g_1\right)^2}, \quad g_1 > 0. \tag{16}$$

Notice that, we assume the noise cannot be ignored in the ST due to the following reasons. First, the noise power at the ST s is same as those in the primary receiver (PR) v and the secondary receiver (SR) d, but the channel fading severity between the primary transmitter (PT) u and the ST s may be much worse than that between u and v, u and d, s and v, s and d, which makes the received signal power (when the PU is active) is comparable with the noise power or smaller than the noise power. Second, for receivers, nodes v and d can use some signal processing methods to reduce the received noise power, such as adaptive filtering and matched filtering [28], while the ST does not use these methods. Finally, the PT u and ST s may be spread spectrum users and the PR v knows the spreading code of u and the SR d knows the spreading code of s. So v and d can use the spread spectrum technology to reduce the noise power to a negligible level. On the other hand, the ST s does not know the spreading code of the PT u (which is a practical scenario), therefore, the spread spectrum technology cannot be used and the noise cannot be ignored. Based on the above reasons, the noise cannot be ignored at the ST and the average received SNR (the ratio between the received signal power the noise power) $\bar{\gamma}$ may be low.

If the existence of the PU's transmission is detected by the SU, i.e. $(\widehat{H}, H_{\mathrm{true}}) = (1, 1)$, the average data rate of the SU is given by (see (17)) where $E(\cdot)$ is the expectation operator and W is the bandwidth of the channel. Δ is given by (see (18)) where $Ei(\cdot)$ is the exponential integral function defined in [25, Eq. 8.211.1].

Proof: Please refer to Appendix 1. □

$$\begin{aligned} R_1 &= E\left\{W \log\left[1 + \frac{\min\left(P_{\max}, I/\left|h_{s,v}\right|^2\right)\left|h_{s,d}\right|^2}{P_u\left|h_{u,d}\right|^2 + N_0}\right]\right\} \\ &= W \exp\left(-\frac{I}{P_{\max}\sigma_1^2}\right)\Delta + \frac{W}{\ln 2}\left[\frac{\dfrac{P_u}{P_{\max}}\ln\dfrac{P_u}{P_{\max}} - \dfrac{\sigma_1^2}{\sigma_2^2}\ln\dfrac{\sigma_1^2}{\sigma_2^2}}{\left(\dfrac{P_u}{P_{\max}} - \dfrac{\sigma_1^2}{\sigma_2^2}\right)} - \ln\left(\frac{P_u}{P_{\max}}\right)\right]\left[1 - \exp\left(-\frac{I}{P_{\max}\sigma_1^2}\right)\right] \end{aligned} \tag{17}$$

$$\begin{aligned} \Delta = \frac{I}{\sigma_2^2 P_u \ln 2}\Bigg\{ &\sum_{n=1}^{+\infty}\frac{1}{n}\Bigg[\sum_{k=0}^{n-1}\binom{n-1}{k}(-1)^{n-1-k}\Bigg[(-1)^{n-k}\frac{\left(\dfrac{I}{\sigma_2^2 P_u}\right)^{n-k-1} Ei\left(-\dfrac{I}{\sigma_1^2 P_{\max}}\right)}{(n-k-1)!} \\ &+ \frac{\exp\left(-\dfrac{I}{\sigma_1^2 P_{\max}}\right)}{\left(\dfrac{P_u\sigma_2^2}{P_{\max}\sigma_1^2}\right)^{n-k-1}}\sum_{q=0}^{n-k-2}\frac{(-1)^q\left(\dfrac{I}{\sigma_1^2 P_{\max}}\right)^q}{(n-k-1)(n-k-2)\ldots(n-k-1-q)}\Bigg]\Bigg]\Bigg\} \end{aligned} \tag{18}$$

When $(\widehat{H}, H_{\text{true}}) = (1, 0)$, the average data rate of the SU is given by

$$\begin{aligned} R_2 &= E\left\{W\log\left[1+\frac{\min\left(P_{\max}, I/|h_{s,v}|^2\right)|h_{s,d}|^2}{N_0}\right]\right\} \\ &= -W\exp\left(-\frac{I}{P_{\max}\sigma_1^2}\right)\frac{I}{\ln(2)(N_0-I)} \\ &\quad\times\left[Ei\left(-\frac{I}{P_{\max}\sigma_1^2}\right)-Ei\left(-\frac{N_0}{P_{\max}\sigma_1^2}\right)\exp\left(\frac{N_0-I}{P_{\max}\sigma_1^2}\right)\right] \\ &\quad - W\frac{\exp\left(\frac{N_0}{P_{\max}\sigma_1^2}\right)Ei\left(-\frac{N_0}{P_{\max}\sigma_1^2}\right)}{\ln(2)}\left[1-\exp\left(-\frac{I}{P_{\max}\sigma_1^2}\right)\right]. \end{aligned} \tag{19}$$

Proof: Please refer to Appendix 2. □

When $(\widehat{H}, H_{\text{true}}) = (0, 0)$, the average data rate of the SU can be calculated as

$$\begin{aligned} R_3 &= E\left\{W\log\left[1+\frac{P_{\max}|h_{s,d}|^2}{N_0}\right]\right\} \\ &= \frac{W}{\ln(2)\sigma_1^2}\int_0^{+\infty}\ln\left(1+\frac{P_{\max}x}{N_0}\right)\exp\left(-\frac{x}{\sigma_1^2}\right)\mathrm{d}x \\ &= -\frac{W}{\ln(2)}\exp\left(\frac{N_0}{P_{\max}\sigma_1^2}\right)Ei\left(-\frac{N_0}{P_{\max}\sigma_1^2}\right) \end{aligned} \tag{20}$$

where the above integral is evaluated with the help of [25, Eq. 4.337.2]. Using (15), when $(\widehat{H}, H_{\text{true}}) = (0, 1)$, the average data rate of the SU is given by

$$\begin{aligned} R_4 &= E\left\{W\log\left(1+\frac{P_{\max}|h_{s,d}|^2}{P_u|h_{u,d}|^2+N_0}\right)\right\} \\ &\simeq \frac{W}{\ln(2)}\int_0^{+\infty}\ln\left(1+\frac{P_{\max}g_1}{P_u}\right)\frac{\sigma_1^2\sigma_2^2}{\left(\sigma_1^2+\sigma_2^2 g_1\right)^2}dg_1 \\ &= \frac{W}{\ln(2)}\left[\frac{\frac{P_u}{P_{\max}}\ln\frac{P_u}{P_{\max}}-\frac{\sigma_1^2}{\sigma_2^2}\ln\frac{\sigma_1^2}{\sigma_2^2}}{\left(\frac{P_u}{P_{\max}}-\frac{\sigma_1^2}{\sigma_2^2}\right)}+\ln\left(\frac{P_{\max}}{P_u}\right)\right]. \end{aligned} \tag{21}$$

Let Ω_i denotes a variable that the probability of the state i, $i \in \{0, 1\}$ lasts for more than Ω_i slots is less than $1-\rho$, where ρ is a predefined threshold. Similar to [17], ρ is set to be 0.99, hence, Ω_i can denote the maximum number of slots that the current state i could last. According to [17], Ω_i is given as

$$\Omega_i = \arg\min_{\phi}\left\{\sum_{k=1}^{\phi}a_{ii}^{k-1}(1-a_{ii}) \geq \rho\right\}, \quad i = 0, 1 \tag{22}$$

where $\sum_{k=1}^{\phi}a_{ii}^{k-1}(1-a_{ii})$ is the probability that the state i lasts for ϕ slots. The expectation of Ω_i is given by

$$\begin{aligned} \Omega_E = E(\Omega_i) &= \left[P(H_0^N)P(H_0|H_0)+P(H_1^N)P(H_0|H_1)\right]\Omega_0 \\ &\quad+\left[P(H_0^N)P(H_1|H_0)+P(H_1^N)P(H_1|H_1)\right]\Omega_1 \end{aligned} \tag{23}$$

where $P(H_i^N)$ is the probability that the PU is in the state i at slot N, which is given by

$$P(H_i^N) = \begin{cases} P(H_i), & t=1 \\ \sum_{j=0}^{1}P(H_j)a_{ji}^{(N)}, & t>1 \end{cases} \tag{24}$$

where $P(H_i)$ is the initial distribution of the state i and $a_{ji}^{(N)}$ is the (j, i) th entry of the N-step transmission matrix $\boldsymbol{A}^N$. Notice that, if the Markov chain is irreducible and all states are aperiodic and positive recurrent, we have $\lim_{t\to\infty}a_{ji}^{(t)} = a_i$, where $a_i > 0$ is a constant and $\sum_i a_i = 1$ [29]. Therefore, there exists an integer t_n that when $t \geq t_n$, $P(H_i^t) \simeq P(H_i^{t+1}) = a_i$. We calculate the $P(H_i^N)$ by using the Matlab with different $(P(H_0), P(H_1))$ when $\boldsymbol{A} = \begin{bmatrix} 0.3 & 0.7 \\ 0.4 & 0.6 \end{bmatrix}$ as shown in Table 1. As shown in Table 1, $P(H_i^N)$ converges fast, i.e. t_n is small ($t_n = 5$).

Table 1 Simulation results of $P(H_i^N)$

N	$P(H_0^N)$	$P(H_1^N)$
1	0.34	0.66
2	0.3660	0.6340
3	0.3634	0.6366
4	0.3637	0.6363
5	0.3636	0.6364
6	0.3636	0.6364

Since the activity of the PU is difficult to be precisely predicted, it may change its state during several consecutive slots. Let X_0 denotes the number of idle slots during Ω consecutive slots. Then, when the current true state of the PU is active, i.e. $H_{\text{true}} = 1$, the expectation of X_0 is given by

$$E(X_0)_{\text{active}} = \begin{cases} \sum_{k=1}^{\Omega}\sum_{m=0}^{\Omega-1}P(X_0=k)k, & \Omega > 1 \\ 0, & \Omega = 1 \end{cases} \tag{25}$$

where m is the number of state changes during Ω slots and the probability $P_(X_0 = k)$ is given as follows [17]: (see (26)) where

$$\begin{aligned} P_1(X_0=k) &= \binom{\frac{k-1}{2}}{\frac{m-1}{2}}\binom{\frac{\Omega-k-1}{2}}{\frac{m-1}{2}} \\ &\quad a_{11}^{\Omega-k}a_{00}^{k}\left(\frac{a_{10}a_{01}}{a_{11}a_{00}}\right)^{(m+1)/2}a_{01}^{-1}, \\ P_2(X_0=k) &= \binom{\frac{k-1}{2}}{\frac{m-2}{2}}\binom{\frac{\Omega-k-1}{2}}{\frac{m}{2}} \\ &\quad a_{11}^{\Omega-k}a_{00}^{k}\left(\frac{a_{10}a_{01}}{a_{11}a_{00}}\right)^{m/2}a_{11}^{-1}. \end{aligned}$$

When the current true state of the PU is idle, i.e. $H_{\text{true}} = 0$, the

$$P(X_0=k) = \begin{cases} P(X_0=k) = P_1(X_0=k) & \text{if } m \text{ is odd, } \frac{m+1}{2} \leq k \leq \Omega-\frac{m+1}{2} \\ P(X_0=k) = P_2(X_0=k) & \text{if } m \text{ is even, } \frac{m}{2} \leq k \leq \Omega-\frac{m+2}{2},\ m>0 \\ 0 & \text{otherwise} \end{cases} \tag{26}$$

IET Commun., 2016, Vol. 10, Iss. 2, pp. 189–198

expectation of X_0 is given by [17]

$$E(X_0)_{\text{idle}} = \begin{cases} \sum_{k=1}^{\Omega}\sum_{m=0}^{\Omega-1} P(X_0=k)k, & \Omega > 1 \\ 1, & \Omega = 1 \end{cases} \tag{27}$$

where (see (28)) where

$$P_3(X_0=k) = \binom{k-1}{\frac{m-1}{2}}\binom{\Omega-k-1}{\frac{m-1}{2}} a_{00}^{k} a_{11}^{\Omega-k}\left(\frac{a_{10}a_{01}}{a_{11}a_{00}}\right)^{(m+1)/2} a_{10}^{-1},$$

$$P_4(X_0=k) = \binom{k-1}{\frac{m}{2}}\binom{\Omega-k-1}{\frac{m-2}{2}} a_{00}^{k} a_{11}^{\Omega-k}\left(\frac{a_{10}a_{01}}{a_{11}a_{00}}\right)^{m/2} a_{00}^{-1}.$$

We will show the accuracy of (25) and (27) in the numerical results provided in Section 4.

If the current sensing result is active, i.e. $\widehat{H}=1$, the ST will employ underlay mode. Then, the average throughput of the SU when adopting the sensing interval Ω, is given by (see (29)) where τ is the length of spectrum sensing time. It is worth remarking that the active state of the PU may not maintain consecutive Ω slots and the true current state of the PU may be idle due to the imperfect characteristics of the spectrum sensing. The transmit power of the SU in underlay mode is less than $P_{\max}$, which is used in interweave mode. Thus, when the current sensing result of the PU is active, using underlay mode may lead to some throughput losses to the SU compared with the case that the activity of the PU is precisely predicted and the proper access mode is adopted. The average decreased throughput of the SU in Ω slots when $\widehat{H}=1$ is given as (see (30)).

If the current decision is idle, i.e. $\widehat{H}=0$, the average possible interference to the PU and the average throughput of the SU are given as follows: (see (31) and (32)). Similar to [17], we calculate the average sensing energy consumption per slot when adopting the sensing interval Ω as

$$f_E(\Omega) = \frac{\varepsilon}{\Omega} \tag{33}$$

where ε is the energy consumption per slot in traditional way, i.e. $\Omega=1$.

3.3 Optimal sensing interval

Obviously, increasing the sensing interval Ω will reduce the average energy consumption for spectrum sensing. However, it will also lead to an increase of decreased throughput of the SU when the current sensing result is active. When the current sensing result is idle, a larger Ω allows the SU to save more energy for spectrum sensing and to enhance the average throughput, at the cost of more interference to the PU. Therefore, there exists a tradeoff among all the aforementioned factors.

Sigmoid function is defined as

$$S(t) = \frac{1}{1+e^{-t}}. \tag{34}$$

The curve of the sigmoid function is shown in Fig. 3. As shown in Fig. 3, it is a monotonically increasing function and $\lim_{t\to+\infty} S(t)=1$. The function is approximately linear in the region [0, 2] and grows with a slow-down tendency in the region $(2,+\infty)$ (non-linear region). We define the region $[0,\ell]$ as the mapping region, which will be used in the subsequent analysis. ℓ is defined as non-linear factor because the proportion of non-linear region in the mapping region is determined by ℓ.

Let $f'_E(f_E(\Omega))$, $f'_{T_{\text{active}}}(f_{T_{\text{active}}}(\Omega))$, $f'_{T_{\text{decrease}}}(f_{T_{\text{decrease}}}(\Omega))$ denote the satisfaction degrees of energy consumption, average throughput of the SU and average decreased throughput of the SU, respectively. The whole satisfaction degrees (WSD) of the SU when the current state of the PU is active is given as

$$f_{\widehat{H}=1}(\Omega) = \omega_{E_{\text{active}}} f'_E(f_E(\Omega)) + \omega_{T_{\text{active}}} f'_{T_{\text{active}}}\left(f_{T_{\text{active}}}(\Omega)\right) + \omega_{T_{\text{decrease}}} f'_{T_{\text{decrease}}}\left(f_{T_{\text{decrease}}}(\Omega)\right) \tag{35}$$

where $\omega_{E_{\text{active}}}$, $\omega_{T_{\text{active}}}$ and $\omega_{T_{\text{decrease}}}$ are weight coefficients. Intuitively, $f'_E(f_E(\Omega))$ should increase with $f_E(\Omega)$ decreases, $f'_{T_{\text{active}}}(f_{T_{\text{active}}}(\Omega))$ should increase with $f_{T_{\text{active}}}(\Omega)$ increases and $f'_{T_{\text{decrease}}}(f_{T_{\text{decrease}}}(\Omega))$ should be a negative value and decrease with $f_{T_{\text{decrease}}}(\Omega)$ increases.

Smaller $f_E(\Omega)$ (larger Ω) leads to an increased satisfaction degree of the energy consumption $f'_E(f_E(\Omega))$, which increases the WSD of the SU. However, it also leads a higher $f_{T_{\text{decrease}}}$, which decreases the WSD [as $f'_{T_{\text{decrease}}}(f_{T_{\text{decrease}}}(\Omega))$ is a negative value and decreased with $f_{T_{\text{decrease}}}$]. Therefore, the satisfaction degree of the energy consumption increases with $1-f_E(\Omega)$, but will not infinitely

$$P(X_0=k) = \begin{cases} P(X_0=k) = P_3(X_0=k) & \text{if } m \text{ is odd, } \frac{m+1}{2} \le k \le \Omega - \frac{m+1}{2} \\ P(X_0=k) = P_4(X_0=k) & \text{if } m \text{ is even, } \frac{m+2}{2} \le k \le \Omega - \frac{m}{2},\ m>0 \\ P(X_0=k) = a_{00}^{\Omega-1} & \text{if } m=0 \\ 0 & \text{otherwise} \end{cases} \tag{28}$$

$$f_{T_{\text{active}}}(\Omega) = P(H_1^N)P(H_1|H_1)\left\{\left[\Omega T - E(X_0)_{\text{active}} T - \tau\right]R_1 + E(X_0)_{\text{active}} TR_2\right\} + P(H_0^N)P(H_1|H_0)\left\{\left[E(X_0)_{\text{idle}} T - \tau\right]R_2 + \left[\Omega - E(X_0)_{\text{idle}}\right]TR_1\right\} \tag{29}$$

$$f_{T_{\text{decrease}}}(\Omega) = P(H_1^N)P(H_1|H_1)E(X_0)_{\text{active}} T(R_3-R_2) + P(H_0^N)P(H_1|H_0)\left[\left(E(X_0)_{\text{idle}}-1\right)T + T - \tau\right](R_3-R_2). \tag{30}$$

$$f_{I_{\text{interference}}}(\Omega) = P(H_1^N)P(H_0|H_1)\left[P_{\max}E\left(|h_{s,v}|^2\right) - I\right]\left[\Omega T - E(X_0)_{\text{active}} T - \tau\right] + P(H_0^N)P(H_0|H_0)\left[P_{\max}E\left(|h_{s,v}|^2\right) - I\right]\left[\Omega - E(X_0)_{\text{idle}}\right]T, \tag{31}$$

$$f_{T_{\text{idle}}}(\Omega) = P(H_1^N)P(H_0|H_1)\left\{E(X_0)_{\text{active}} TR_3 + \left[\Omega T - E(X_0)_{\text{active}} T - \tau\right]R_4\right\} + P(H_0^N)P(H_0|H_0)\left\{\left[E(X_0)_{\text{idle}} T - \tau\right]R_3 + \left[\Omega - E(X_0)_{\text{idle}}\right]TR_4\right\}. \tag{32}$$

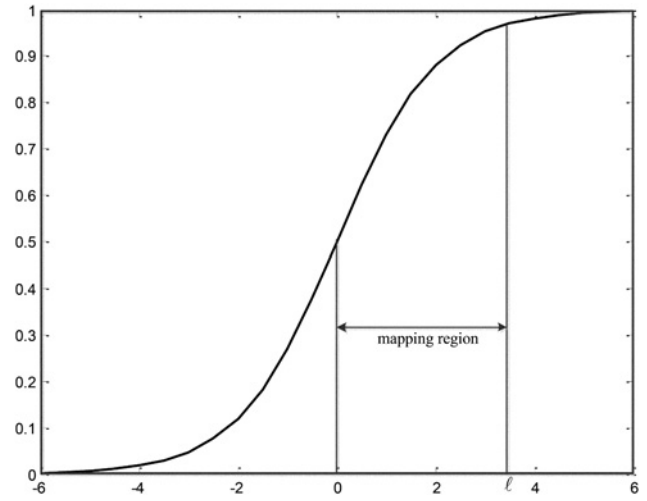

Fig. 3 *Sigmoid function*

increase. The increasing tendency should slow-down in large $1 - f_E(\Omega)$ region. From Fig. 3, it's not hard to see that the sigmoid function can describe the tendency of $f'_E(f_E(\Omega))$ very well by mapping [0, max $(1 - f_E(\Omega))$] to the region [0, ℓ], where ℓ is determined by the requirement of users. The cases of $f'_{T_{\text{active}}}(f_{T_{\text{active}}}(\Omega))$, $f'_{T_{\text{decrease}}}(f_{T_{\text{decrease}}}(\Omega))$ and when the current state of the PU is idle can be analysed similarly. For convenience, we replace $f'_E(f_E(\Omega))$, $f'_{T_{\text{active}}}(f_{T_{\text{active}}}(\Omega))$, $f'_{T_{\text{decrease}}}(f_{T_{\text{decrease}}}(\Omega))$ by $f'_E(\Omega)$, $f'_{T_{\text{active}}}(\Omega)$, $f'_{T_{\text{decrease}}}(\Omega)$, respectively.

If the spectrum sensing is perfect, $\Omega_{\max}$ should be set as Ω_i when $\widehat{H} = i$. However, since the spectrum sensing is imperfect in our paper, the ST does not have perfect information about the current state of the PU. Thus, we set $\Omega_{\max}$ as Ω_E to compromise the impact of the imperfect spectrum sensing.

According to the analysis above, the satisfaction degrees of the factors when $\widehat{H} = 1$ are given as

$$f'_E(\Omega) = \frac{1}{1 + \exp\left[-\ell\left(1 - \widetilde{f}_E(\Omega)\right)\right]} \tag{36}$$

$$f'_{T_{\text{active}}}(\Omega) = \frac{1}{1 + \exp\left[-\ell\widetilde{f}_{T_{\text{active}}}(\Omega)\right]} \tag{37}$$

$$f'_{T_{\text{decrease}}}(\Omega) = -\frac{1}{1 + \exp\left[-\ell\widetilde{f}_{T_{\text{decrease}}}(\Omega)\right]} \tag{38}$$

where

$$\widetilde{f}_E(\Omega) = \frac{f_E(\Omega)}{\max\limits_{1\le\Omega\le\Omega_{\max}}[f_E(\Omega)]},$$

$$\widetilde{f}_{T_{\text{active}}}(\Omega) = \frac{f_{T_{\text{active}}}(\Omega)}{\max\limits_{1\le\Omega\le\Omega_{\max}}[f_{T_{\text{active}}}(\Omega)]} \text{ and}$$

$$\widetilde{f}_{T_{\text{decrease}}}(\Omega) = \frac{f_{T_{\text{decrease}}}(\Omega)}{\max\limits_{1\le\Omega\le\Omega_{\max}}[f_{T_{\text{decrease}}}(\Omega)]}.$$

The reasons for normalising are as follows. First, normalising can prevent the term exp (·) form overflow and underflow. Second, in order to map the ranges of each term to [0, ℓ], each term must be normalised to the range of [0, 1].

Table 2 Simulation parameters and acronyms

Parameter	Value
σ_1^2	5 dB
σ_2^2	3 dB
P_u	6 dBW
$P_{\max}$	5 dBW
I	4 dBW
N_0	−10 dBW
ρ	0.99
ℓ	4
$\boldsymbol{A}$	$\begin{bmatrix} 0.3 & 0.7 \\ 0.4 & 0.6 \end{bmatrix}$
W	200 kHz
f_s	1 MHz
$[P(H_0), P(H_1)]$	[0.6, 0.4]
T	20ms
τ	1 ms (unless otherwise stated)
ε	$0.1 \times \tau W$
N	10
$\omega_{E_{\text{idle}}}, \omega_{T_{\text{idle}}}, \omega_{I_{\text{interference}}}, \omega_{E_{\text{active}}}, \omega_{T_{\text{active}}}, \omega_{T_{\text{decrease}}}$	[1, 10]
Acronyms	
CI	conventional spectrum sensing scheme using interweave mode
CH	conventional spectrum sensing scheme using hybrid mode
PRH	proposed hybrid interweave/underlay mode spectrum sensing scheme
ANSS	average number of times that the spectrum sensing is performed per time slot

When $\widehat{H} = 1$, the optimisation problem is given by

$$\begin{aligned} \Omega^* &= \arg\max f_{\widehat{H}=1}(\Omega) \\ &\text{s.t. } 1 \le \Omega \le \Omega_{\max}. \end{aligned} \tag{39}$$

Similar to (35)–(39), when the current sensing result is idle, the optimisation problem is formulated by replacing the subscript $\widehat{H} = 1$, T_{active} and T_{decrease} with $\widehat{H} = 0$, T_{idle} and $I_{\text{interference}}$, respectively.

Generally, $\Omega_{\max}$ will not be very large. Therefore, the optimal sensing interval Ω^* can be obtained by one-dimensional exhaustive search over [1, $\Omega_{\max}$], the complexity of the phase of search is $O(\Omega_{\max})$. Since M is usually much larger than $\Omega_{\max}$, the complexity of the optimal problem is $O(M)$.

4 Numerical results

In this section, we present numerical results for our proposed sensing scheme with the help of Matlab. The simulation scenario is set according to the channel model, which is shown in Fig. 1. Table 2 lists the simulation parameters and acronyms. Some of them are set according to [17, 30].

The analytical and simulation results for the expected number of idle slots in consecutive Ω slots are shown in Fig. 4. The analytical results obtained by using (25) and (27) match well with the simulation results, which verify our analysis in Section 3.2.

Figs. 5 and 6 show the optimal sensing interval when the current sensing result of the SU is idle and active, respectively. The weight coefficients are set as $[\omega_{E_{\text{idle}}}, \omega_{T_{\text{idle}}}, \omega_{T_{\text{decrease}}}] = [\omega_{E_{\text{active}}}, \omega_{T_{\text{active}}}, \omega_{T_{\text{interefrence}}}] = [3, 4, 5]$. It can be observed that when the current decision is idle, i.e. $\widehat{H} = 0$, $f'_{T_{\text{idle}}}(\Omega)$ and $f'_{E_{\text{idle}}}(\Omega)$ increase with Ω while $f'_{I_{\text{interference}}}(\Omega)$ decreases with Ω. The reason is that as sensing interval increases, the energy consumption per slot becomes smaller and the throughput of the SU goes larger and the SU will also produce more interference to the PU. Thus, it results in a higher satisfaction degree on both the energy consumption, the throughput, but a lower satisfaction degree on the interference to the PU. Besides, Fig. 6 shows that satisfaction degree $f'_{T_{\text{active}}}(\Omega)$

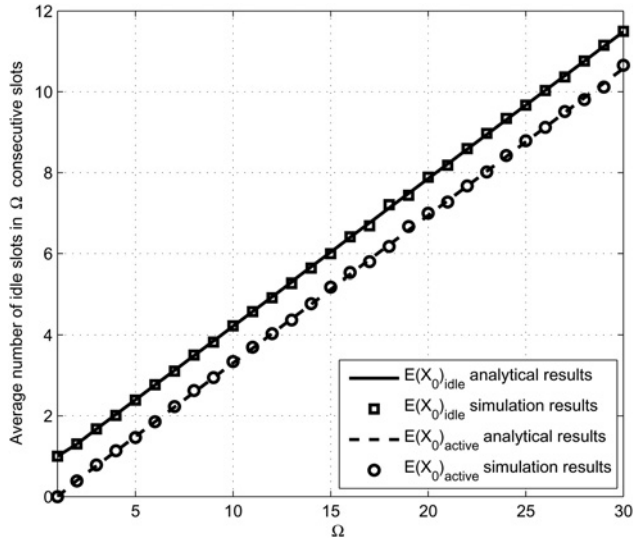

Fig. 4 *Expected number of idle slots in consecutive Ω slots*

and $f'_{E_{\text{active}}}(\Omega)$ increase with Ω while $f'_{I_{\text{decrease}}}(\Omega)$ decreases with Ω. The reasons for this phenomenon are similar to that of Fig. 5. Another interesting observation is: although the weight coefficients are same, the optimal sensing interval may be different from different current sensing results. As shown in Figs. 5 and 6, the optimal intervals are 2 and 3 for $\widehat{H}=0$ and $\widehat{H}=1$, respectively.

Figs. 7 and 8 show the effect of the weight coefficients on the optimal spectrum sensing interval. There are three weight coefficients for both $\widehat{H}=0$ and $\widehat{H}=1$, which can be adjusted to satisfy different requirements of the PU and the SU. For example, if the SU want to save more energy consumed for spectrum sensing, it can improve the weight coefficient of energy consumption satisfaction degree to choose a larger sensing interval. As shown in Figs. 7 and 8, for given $\omega_{I_{\text{interference}}}$ and $\omega_{T_{\text{decrease}}}$, Ω* increases with $\omega_{E_{\text{idle}}}$ and $\omega_{E_{\text{active}}}$, respectively. Another obvious phenomenon is that Ω* decreases with $\omega_{T_{\text{interference}}}$ and $\omega_{T_{\text{decrease}}}$, which matches our analysis that if the PU is more sensitive to the interference, the SU can increase the $\omega_{T_{\text{interference}}}$ to sense the PU more frequently. The case of $\omega_{T_{\text{decrease}}}$ can be explained similarly.

To compare our work with the conventional spectrum sensing scheme, we consider two conventional cases: the ST adopts interweave mode and performs spectrum sensing at each slot with sensing time τ and the ST adopts hybrid interweave/underlay

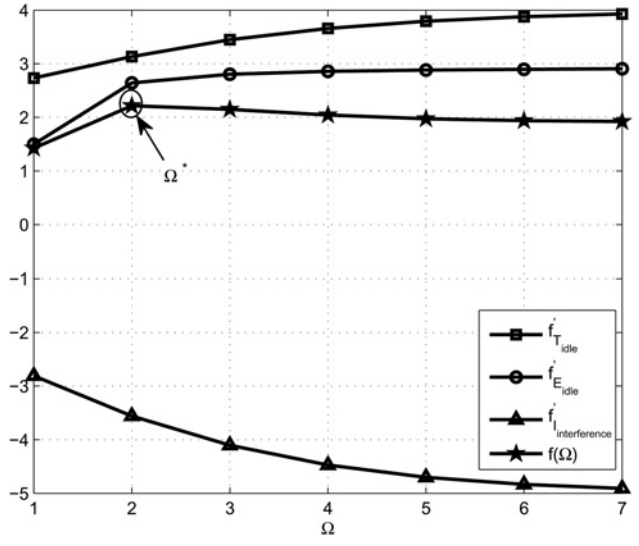

Fig. 5 *Optimal spectrum sensing interval when* $\widehat{H}=0$, $[\omega_{E_{idle}}, \omega_{T_{idle}}, \omega_{T_{decrease}}]=[3, 4, 5]$

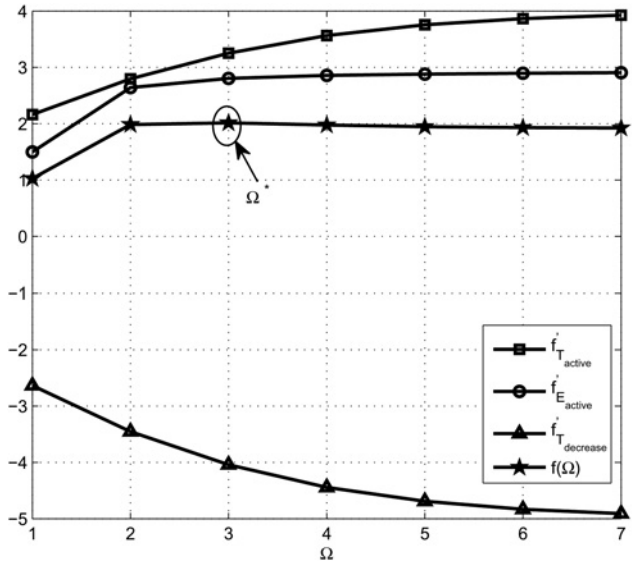

Fig. 6 *Optimal spectrum sensing interval when* $\widehat{H}=1$, $[\omega_{E_{active}}, \omega_{T_{active}}, \omega_{T_{interefrence}}]=[3, 4, 5]$

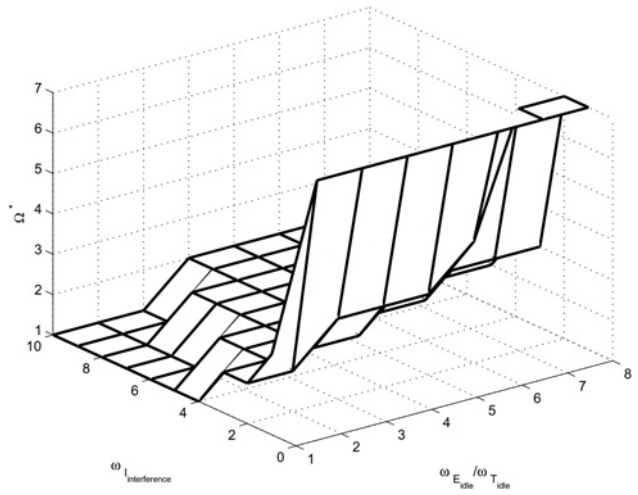

Fig. 7 *Effect of the weight coefficients when* $\widehat{H}=0$, $\omega_{T_{idle}}=1$

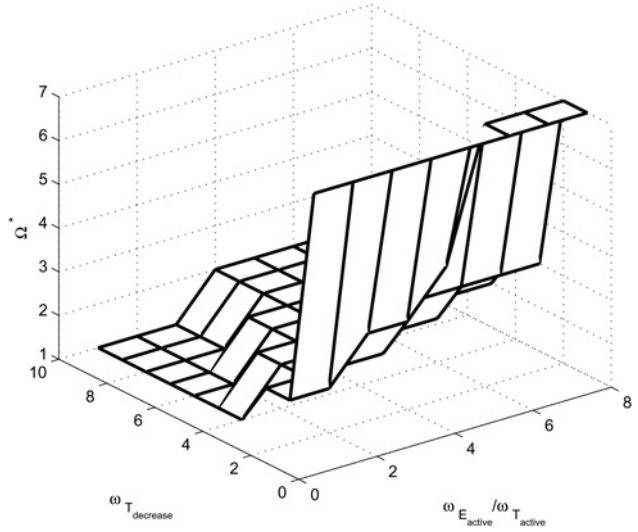

Fig. 8 *Effect of the weight coefficients when* $\widehat{H}=1$, $\omega_{T_{active}}=1$

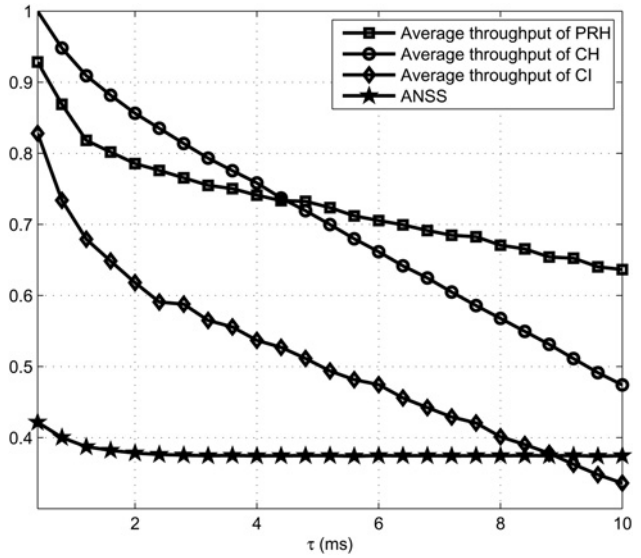

Fig. 9 *Comparison with the conventional spectrum sensing scheme*

mode and performs spectrum sensing at each slot with sensing time τ. For convenience, we use the acronyms provided in Table 2 to denote the cases above. One of the advantages of our proposed scheme is that the ST only needs to sense the PU once from slot t to slot $t+\Omega^*-1$ and transmit $(\Omega^*-1)\tau$ longer than the conventional scheme. Intuitively, the longer the sensing time τ is, the more advanced the proposed sensing scheme is. Fig. 9 verifies our analysis. As shown in Fig. 9, the throughput of proposed hybrid interweave/underlay mode spectrum sensing scheme (PRH) is higher than that of CH when τ is relatively large. When τ is relatively small, the CH is superior. This is because that the PU may change its state during slot t to slot $t+\Omega^*-1$, which results in the inequality between the actual throughput and the expected throughput. For example, we assume the PU is active at slot t and idle at slot $t+1$ to $t+\Omega^*-1$. In PRH case, the ST will adopt underlay mode and transmit Ω^* consecutive slots, the maximum throughput obtained by the SU is $t_{\mathrm{PRH}}(\tau)=R_1\times(T-\tau)+R_2\times(\Omega^*-1)T$, while in CH case, the maximum obtained throughput is $t_{\mathrm{CH}}(\tau)=R_1\times(T-\tau)+R_3\times(\Omega^*-1)(T-\tau)$. Let $\Upsilon=\dfrac{t_{\mathrm{PRH}}(\tau)}{t_{\mathrm{CH}}(\tau)}=\dfrac{R_2}{R_3}\times\dfrac{T}{(T-\tau)}$, where $R_2/R_3<1$ [as shown in (19) and (20)]. Obviously, Υ will larger than 1 ($t_{\mathrm{PRH}}(\tau)>t_{\mathrm{CH}}(\tau)$) when τ is relatively large. Another phenomenon in Fig. 9 is that throughput of PRH is higher than that of CI at all τ, which is unexpected because hybrid interweave/underlay mode can use the spectrum more thoroughly. Fig. 9 also shows that the ANSS decreases with τ and changes a little with the increase of τ when τ is relatively large. We denote the optimal sensing interval at different current sensing results as $\Omega^*_{H=i}$, $i\in\{0,1\}$. In our simulation environment, $\Omega^*_{H=0}=2$ and $\Omega^*_{H=1}=3$. Larger sensing time τ leads to a higher detection probability, i.e. more active states will be detected with the increase of τ. Therefore, the ST will sense the PU more infrequently with the increase of τ (because $\Omega^*_{H=0}<\Omega^*_{H=1}$), which results in the decrease of the curve in small τ region. When τ is relatively large, the detection probability tends to 1 and changes a little with τ increases, which is the reason for the tendency of the curve in large τ region.

5 Conclusions

In this paper, we investigated the problem of optimal spectrum sensing interval under the condition of imperfect spectrum sensing over Rayleigh fading channels. An HMM was used to model the sensing process. The optimal sensing interval was obtained by exploring the balance among the average energy consumption for spectrum sensing, the average throughput of the SU and the average interference to the PU. Most results, e.g. the average throughput of the SU and the average interference to the PU were derived in closed form. Simulation results confirmed the analysis and showed that our proposed algorithm can satisfy different requirements of the SU by adjusting the weight coefficients.

6 Acknowledgment

This work was supported by the National Natural Science Foundation of China (61301179), the Doctorial Programs Foundation of the Ministry of Education (20110203110011) and the 111 Project (B08038).

7 References

1 Dohler, M., Heath, R., Lozano, A., *et al.*: 'Is the PHY layer dead?', *IEEE Commun. Mag.*, 2011, **49**, (4), pp. 159–165
2 FCC: 'Spectrum policy task force report', ET Docker 02-155, November 2002
3 Mitola, J., Maguire, G.Q.: 'Cognitive radio: making software radios more personal', *IEEE Pers. Commun.*, 1999, **6**, (4), pp. 13–18
4 Haykin, S.: 'Cognitive radio: Brain-empowered wireless communications', *IEEE J. Sel. Areas Commun.*, 2005, **23**, (2), pp. 201–220
5 Yucek, T., Arslan, H.: 'A survey of spectrum sensing algorithms for cognitive radio applications', *IEEE Commun. Surv. Tutor.*, 2009, **11**, (1), pp. 116–130
6 Liu, J., Li, Z.: 'Lowering the signal-to-noise ratio wall for energy detection using parameter-induced stochastic resonator', *IET Commun.*, 2015, **9**, (1), pp. 101–107
7 Li, B., Li, X.F., Nallanathan, A., *et al.*: 'Energy detection based spectrum sensing for cognitive radios over time-frequency doubly selective fading channels', *IEEE Trans. Signal Process.*, 2014, **63**, (2), pp. 402–417
8 López-Benítez, M., Casadevall, F.: 'Improved energy detection spectrum sensing for cognitive radio', *IET Commun.*, 2012, **6**, (8), pp. 785–796
9 Gardner, W.A.: 'Exploitation of spectral redundancy in cyclostationary signals', *IEEE Signal Process. Mag.*, 1991, **8**, (2), pp. 14–36
10 Zeng, Y., Liang, Y.C.: 'Eigenvalue-based spectrum sensing algorithms for cognitive radio', *IEEE Trans. Commun.*, 2009, **57**, (6), pp. 1784–1793
11 Mishra, S.M., Sahai, A., Brodersen, R.W.: 'Cooperative sensing among cognitive radios'. Proc. IEEE ICC, Istanbul, Turkey, June 2006, pp. 1658–1663
12 Quan, Z., Cui, S., Poor, H.V., *et al.*: 'Collaborative wideband sensing for cognitive radios', *IEEE Signal Process. Mag.*, 2008, **25**, (6), pp. 60–73
13 Chaudhari, S., Lunden, J., Koivunen, V., *et al.*: 'Cooperative sensing with imperfect reporting channels: hard decisions or soft decisions?', *IEEE Trans. Signal Process.*, 2012, **60**, (1), pp. 18–28
14 Srinivasa, S., Jafar, S.: 'Cognitive radios for dynamic spectrum access the throughput potential of cognitive radio: a theoretical perspective', *IEEE Commun. Mag.*, 2007, **45**, (5), pp. 73–79
15 Goldsmith, A., Jafar, S.A., Maric, I., *et al.*: 'Breaking spectrum gridlock with cognitive radios: an information theoretic perspective', *Proc. IEEE*, 2009, **97**, (5), pp. 894–914
16 Willkomm, D., Machiraju, S., Bolot, J., *et al.*: 'Primary user behavior in cellular networks and implications for dynamic spectrum access', *IEEE Commun. Mag.*, 2009, **47**, (3), pp. 88–95
17 Xing, X.S., Jing, T., Li, H., *et al.*: 'Optimal spectrum sensing interval in cognitive radio networks', *IEEE Trans. Parallel Distrib. Syst.*, 2013, **25**, (9), pp. 2408–2417
18 Ghosh, C., Cordeiro, C., Agrawal, D., *et al.*: 'Markov chain existence and hidden Markov models in spectrum sensing', *IEEE Pervasive Comput. Commun.*, 2009, pp. 1–6
19 Rabiner, L.R.: 'A tutorial on hidden Markov models and selected applications in speech recognition', *Proc. IEEE*, 1989, **77**, (2), pp. 257–286
20 Treeumnuk, D., Popescu, D.C.: 'Using hidden Markov models to evaluate performance of cooperative spectrum sensing', *IET Commun.*, 2013, **7**, (17), pp. 1969–1973
21 Nguyen, T., Mark, B.L., Ephraim, Y.: 'Spectrum sensing using a hidden bivariate Markov model', *IEEE Trans. Wirel. Commun.*, 2013, **12**, (9), pp. 4582–4591
22 Chen, Z., Hu, Z., Qiu, R.: 'Quickest spectrum detection using hidden Markov model for cognitive radio'. Proc. IEEE Military Communications Conf. (MILCOM), Boston, USA, October 2009, pp. 1–7
23 Stamp, M.: 'A Revealing Introduction to Hidden Markov Models', 2012, Available at http://www.cs.sjsu.edu/%7Estamp/RUA/HMM.pdf
24 Digham, F.F., Alouini, M.-S., Simon, M.K.: 'On the energy detection of unknown signals over fading channels'. Proc. IEEE ICC, Anchorage, AK, USA, May 2003, pp. 3575–3579
25 Gradshteyn, I.S., Ryzhik, I.M.: 'Table of integrals, series, and products' (Academic Press, San Diego, CA, 2000, 6th edn.)
26 Harsini, J.S., Zorzi, M.: 'Transmission strategy design in cognitive radio systems with primary ARQ control and QoS provisioning', *IEEE Trans. Commun.*, 2014, **62**, (6), pp. 1790–1802
27 Kwan, R., Leung, C.: 'Gamma variate ratio distribution with application to CDMA performance analysis'. Proc. IEEE Symp. Advanced Wired/Wireless Communication, Princeton, NJ, USA, April 2005, pp. 188–191
28 Simon, M.K., Alouini, M.S.: 'Digital Communication over Fading Channels' (Wiley-IEEE Press, 2004, 2nd edn.)
29 Grimmett, G.R., Stirzaker, D.R.: 'Probability and Random Processes' (Oxford University Press, 2001)

30 Peh, E., Liang, Y.C., Guan, Y.L., *et al.*: 'Energy-efficient cooperative spectrum sensing in cognitive radio networks'. Proc. IEEE GLOBECOM, Houston, TX, USA, 2011, pp. 1–5

8 Appendices

8.1 Appendix 1

Derivation of the average data rate R_1: let $Z = \min(P_{\max}, I/|h_{s,v}|^2)$, which is a random variable, the cumulative distribution function of Z is given by

$$F_Z(z) = \begin{cases} \mathrm{P}\left(\dfrac{I}{|h_{s,v}|^2} \le z\right), & 0 < z < P_{\max} \\ 1, & z \ge P_{\max} \end{cases} = \begin{cases} \exp\left(-\dfrac{I}{z\sigma_{s,v}^2}\right), & z < P_{\max} \\ 1, & z \ge P_{\max}. \end{cases} \tag{40}$$

Notice that, Z is neither a continuous random variable nor a discrete random variable. When $Z < P_{\max}$, Z is a continuous random variable with the PDF given by

$$f_Z(z) = \frac{I}{z^2\sigma_{s,v}^2}\exp\left(-\frac{I}{z\sigma_{s,v}^2}\right) = \frac{I}{z^2\sigma_1^2}\exp\left(-\frac{I}{z\sigma_1^2}\right), \quad 0 < z < P_{\max}. \tag{41}$$

The probability of $Z \in (0, P_{\max})$ can be calculated as

$$\mathrm{P}(0 < Z < P_{\max}) = \int_0^{P_{\max}} \frac{I}{z^2\sigma_1^2} \exp\left(-\frac{I}{z\sigma_1^2}\right) \mathrm{d}z = \exp\left(-\frac{I}{P_{\max}\sigma_1^2}\right). \tag{42}$$

Therefore, the probability of $Z = P_{\max}$ is given by

$$P(Z = P_{\max}) = 1 - \exp\left(-\frac{I}{P_{\max}\sigma_1^2}\right). \tag{43}$$

Using (15), we have

$$\log\left[1 + \frac{\min\left(P_{\max}, I/|h_{s,v}|^2\right)|h_{s,d}|^2}{P_u|h_{u,d}|^2 + N_0}\right] \simeq \log\left[1 + \frac{\min\left(P_{\max}, I/|h_{s,v}|^2\right)G_1}{P_u}\right]. \tag{44}$$

where $G_1 = |h_{s,d}|^2/|h_{u,d}|^2$.

Let

$$J_1 = W\log\left[1 + \frac{\min\left(P_{\max}, I/|h_{s,v}|^2\right)|h_{s,d}|^2}{P_u|h_{u,d}|^2 + N_0}\right],$$

the conditional expectation of J_1 given $Z \in (0, P_{\max})$ can be calculated as

$$E[J_1|Z \in (0, P_{\max})] = W\int_0^{P_{\max}}\int_0^{+\infty} \log\left(1 + \frac{zg_1}{P_u}\right) \frac{\sigma_1^2\sigma_2^2}{\left(\sigma_1^2 + \sigma_2^2 g_1\right)^2}\frac{I}{z^2\sigma_1^2}\exp\left(-\frac{I}{z\sigma_1^2}\right)\mathrm{d}g_1\,\mathrm{d}z$$

$$= \frac{IW\sigma_2^2}{\ln 2}\int_0^{P_{\max}} \frac{1}{\sigma_1^2\sigma_2^2}\left[\frac{\frac{P_u}{z}\ln\frac{P_u}{z} - \frac{\sigma_1^2}{\sigma_2^2}\ln\frac{\sigma_1^2}{\sigma_2^2}}{\left(\frac{P_u}{z} - \frac{\sigma_1^2}{\sigma_2^2}\right)} - \ln\left(\frac{P_u}{z}\right)\right] \frac{1}{z^2}\exp\left(-\frac{I}{z\sigma_1^2}\right)\mathrm{d}z$$

$$\underline{y = \frac{P_u}{z}, \quad c = \frac{I}{\sigma_2^2 P_u}}$$

$$b = \frac{\sigma_1^2}{\sigma_2^2}, \quad u = \frac{y}{b}\,\frac{cW}{\ln 2}\int_{\frac{P_u}{bP_{\max}}}^{+\infty} \frac{\ln u}{(u-1)}\exp(-cu)\mathrm{d}u \tag{45}$$

Using

$$\ln x = \sum_{k=1}^{+\infty}\frac{1}{k}\left(\frac{x-1}{x}\right)^k, \quad (1+x)^n = \sum_{k=0}^{n}\binom{n}{k}x^k,$$

and with the help of [25, Eq. 3.351.4], (45) becomes

$$E[J_1|Z \in (0, P_{\max})] = \frac{WI}{\sigma_2^2 P_u \ln 2} \left\{\sum_{n=1}^{+\infty}\frac{1}{n}\left[\sum_{k=0}^{n-1}\binom{n-1}{k}(-1)^{n-1-k}\left[(-1)^{n-k}\right.\right.\right.$$

$$\left.\left.\left.\frac{\left(\frac{I}{\sigma_2^2 P_u}\right)^{n-k-1} Ei\left(-\frac{I}{\sigma_1^2 P_{\max}}\right)}{(n-k-1)!} + \frac{\exp\left(-\frac{I}{\sigma_1^2 P_{\max}}\right)}{\left(\frac{P_u\sigma_2^2}{P_{\max}\sigma_1^2}\right)^{n-k-1}}\right.\right.\right.$$

$$\left.\left.\left.\sum_{q=0}^{n-k-2}\frac{(-1)^q\left(\frac{I}{\sigma_1^2 P_{\max}}\right)^q}{(n-k-1)(n-k-2)\ldots(n-k-1-q)}\right]\right]\right\} \tag{46}$$

The conditional expectation of R given $Z = P_{\max}$ is calculated as

$$E[J_1|Z = P_{\max}] = W\int_0^{+\infty}\log\left(1 + \frac{P_{\max}g_1}{P_u}\right)\frac{\sigma_1^2\sigma_2^2}{\left(\sigma_1^2 + \sigma_2^2 g_1\right)^2}\mathrm{d}g_1 = \frac{W}{\ln 2}\left[\frac{\frac{P_u}{P_{\max}}\ln\frac{P_u}{P_{\max}} - \frac{\sigma_1^2}{\sigma_2^2}\ln\frac{\sigma_1^2}{\sigma_2^2}}{\left(\frac{P_u}{P_{\max}} - \frac{\sigma_1^2}{\sigma_2^2}\right)} - \ln\left(\frac{P_u}{P_{\max}}\right)\right]. \tag{47}$$

Therefore, the expectation of R is given by

$$R_1 = E(J_1) = E[J_1|Z \in (0, P_{\max})]P[Z \in (0, P_{\max})] + E[J_1|Z = P_{\max}]P(Z = P_{\max}). \tag{48}$$

Substituting (42), (43), (46), (47) into (48), we have (17).

8.2 Appendix 2

Derivation of R_2: let

$$J_2 = W \log\left[1 + \frac{\min\left(P_{\max}, I/|h_{s,v}|^2\right)|h_{s,d}|^2}{N_0}\right].$$

Following the similar procedure as in Appendix 1, we have

$$\begin{aligned} E\left[J_2|Z \in (0, P_{\max})\right] &= W \int_0^{P_{\max}} \int_0^{+\infty} \log\left(1 + \frac{zx}{N_0}\right) \\ &\frac{1}{\sigma_1^2}\exp\left(-\frac{x}{\sigma_1^2}\right)\frac{I}{z^2\sigma_1^2}\exp\left(-\frac{I}{z\sigma_1^2}\right) \mathrm{d}x\, \mathrm{d}z \\ &= \frac{IW}{\sigma_1^2}\frac{1}{\ln(2)}\int_0^{P_{\max}} e^{\frac{N_0}{z\sigma_1^2}} Ei\left(-\frac{N_0}{z\sigma_1^2}\right)\frac{-1}{z^2}\exp\left(-\frac{I}{z\sigma_1^2}\right) \mathrm{d}z \\ &= -\frac{IW}{\ln(2)(N_0 - I)} \\ &\left[Ei\left(-\frac{I}{P_{\max}\sigma_1^2}\right) - Ei\left(-\frac{N_0}{P_{\max}\sigma_1^2}\right)\exp\left(\frac{N_0 - I}{P_{\max}\sigma_1^2}\right)\right]. \end{aligned} \quad (49)$$

The above integral is evaluated with the help of [25, Eq. 4.337.2] and [25, Eq. 3.351.4]. The $E[J_2|Z = P_{\max}]$ is given as

$$E\left[J_2|Z = P_{\max}\right] = -\frac{\exp\left(N_0/P_{\max}\sigma_1^2\right)Ei\left(-N_0/P_{\max}\sigma_1^2\right)}{\ln(2)} \quad (50)$$

Then, the $R_2 = E(J_2)$ can be calculated as

$$\begin{aligned} R_2 = E(J_2) &= E[J_2|Z \in (0, P_{\max}).]P[Z \in (0, P_{\max})] \\ &+ E[J_2|Z = P_{\max}.]P(Z = P_{\max}). \end{aligned} \quad (51)$$

Substituting (42), (43), (49), (50) into (51), we have (19).

IET Commun., 2016, Vol. 10, Iss. 2, pp. 189–198